Systems pharmacology of the amyloid cascade : unfolding oligomer modulation in Alzheimer's disease

Maanen, E.M.T. van

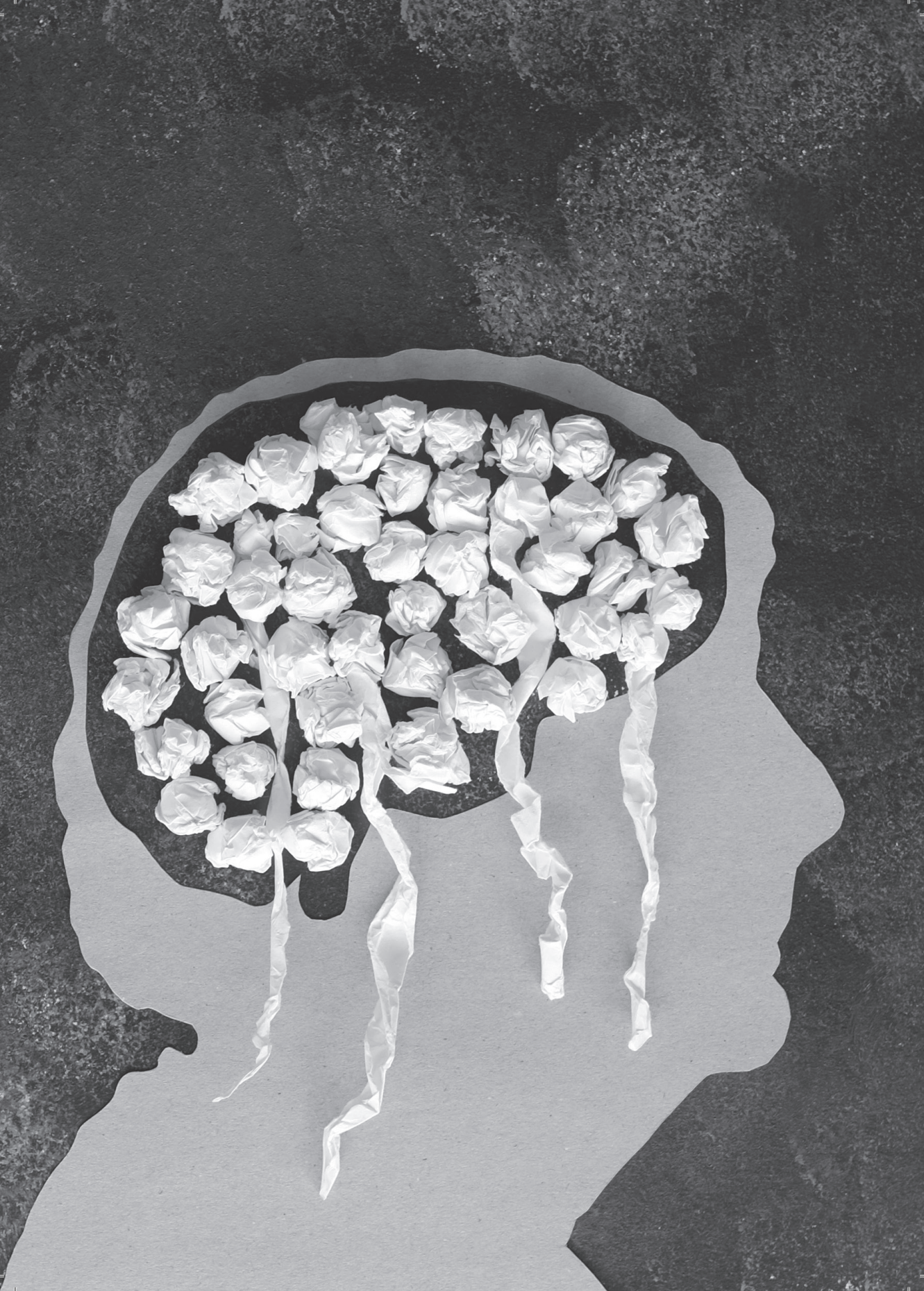

Chapter 4

Integrating tracer kinetic data in a systems pharmacology model of the amyloid precursor pathway: effect of a β-secretase inhibitor

E.M.T. van Maanen, T.J. van Steeg, J.A. Dobrowolska Zakaria,
M.S. Michener, M.J. Savage, M.E. Kennedy, R.J. Bateman,
H.J. Kleijn, J.A. Stone, M. Danhof

Abstract

Purpose: To assess the ability of a recently developed systems pharmacology model of the β-amyloid precursor protein (APP) pathway to predict the tracer kinetics of APP metabolites following administration of a β-secretase inhibitor.

Methods: A stable isotope tracer $^{13}C_6$-labelled Leucine was administered to cisterna magna ported (CMP) rhesus monkeys in conjunction with the β-secretase (BACE1) inhibitor MBi-5. The fraction labelled APP metabolites (total Aβ, sAPPα , sAPPβ) were measured over 145 hours. A systems pharmacology model of the APP pathway, recently developed using information on CSF absolute concentrations of the APP metabolites (Aβ40, Aβ42, sAPPβ and sAPPα), was used as the basis for the prediction of the tracer kinetic data.

Results: BACE1 inhibition by MBi-5 resulted in a concentration driven saturable effect on the APP pathway as reflected in the absolute concentrations of the metabolites, fraction labelled Aβ and sAPPβ. In contrast, this MBi-5 concentration dependency was not observed in the fraction labelled sAPPα because similar drug effects on both the labelled and unlabelled pools for this marker yield a lack of dose-differentiation in this relative biomarker. The recent APP systems model and absolute concentrations of the APP metabolites support a dose-dependent response. The current results indicate that interpretation of fraction labelled data is complex and best achieved with a kinetic model. Aβ40 and Aβ42 dynamics did not fully explain the measured fraction labelled Aβ. The model was used to demonstrate that a contribution of other Aβ isoforms with altered dynamics from Aβ40 and Aβ42 is a potential explanation.

Conclusions: This analysis demonstrated that using a systems pharmacology model to integrate tracer kinetic data with absolute protein concentrations enables a more accurate interpretation of the tracer kinetic data.

Key words

Systems pharmacology - APP pathway - tracer kinetics - Aβ - β-secretase inhibition

Introduction

The accumulation of amyloid-β (Aβ) peptide in the brain parenchyma as result of overproduction and/or decreased clearance has been implicated in the pathophysiology of Alzheimer's disease (AD)[1]. Toxic soluble Aβ oligomers (Aβ_O) are considered to be the drivers of the neurodegeneration in the brains of patients with AD[2]. Modulation of Aβ is a therapeutic target for AD, with the potential for eliciting a disease modifying effect by reducing high levels of Aβ peptides and subsequently preventing the development of Aβ associated pathologies[3,4]. One of the main therapeutic strategies aims at Aβ reduction through the inhibition of secretases responsible for their production.

Aβ peptides are generated by two sequential proteolytic cleavages of the β-amyloid precursor protein (APP)[5]. The first step is catalyzed by β-site APP-cleaving enzyme (BACE1, also called β-secretase) to yield the N-terminal fragment soluble APPβ (sAPPβ) and the C-terminal membrane-bound 99-aminoacid fragment (C99). C99 undergoes further cleavage by a second protease known as γ-secretase to generate Aβ species of different chain lengths, the major variants having 38 (Aβ38), 40 (Aβ40) or 42 (Aβ42) amino acids[6]. A third protease, α-secretase, cleaves APP within the Aβ sequence generating non-amyloidogenic soluble APPα (sAPPα) and precluding the formation of the major Aβ variants[7]. A new APP processing pathway was recently reported by Willem et al. (2015), in which sequential cleavage of APP by η-secretase and BACE1 or ADAM10 leads to the formation of A$\eta - \beta$ and A$\eta - \alpha$, respectively. There may be other alternate pathways unknown at this time.

To improve the prediction of therapeutic effects on Aβ burden, an understanding of the behaviour of the APP system as a whole, as opposed to the behaviour of its individual components, is imperative. This requires a quantitative analysis of the dynamic interactions between drugs and the APP processing pathway. To this end, a systems pharmacology model of the APP processing pathway was reported recently[9].

The model was based on the absolute concentrations of APP metabolites sAPPα, sAPPβ, Aβ40 and Aβ42 and described their kinetics and interrelationships following β-secretase inhibition. In the current analysis, we evaluated whether the systems pharmacology model could adequately describe the tracer kinetic data of the APP metabolites following β-secretase inhibition.

Tracer kinetic studies have been introduced to gain understanding of the dynamics of the APP pathway following secretase inhibition. In 2007 Bateman et al.[10] published a stable isotope labeling kinetics (SILK) protocol for quantification of Aβ production

and clearance rates in the brain. In short, a tracer is infused intravenously after drug administration and the proportion of synthesized labelled APP metabolites is monitored for 145 hours. The SILK protocol measures the fraction of APP metabolites labelled with tracer. In addition, many of the SILK studies used liquid chromatography/MS or enzyme linked immunosorbant assay (ELISA) to measure absolute APP metabolite concentrations[11,12,13]. Integrating the tracer kinetic data with absolute protein concentration measurements yields detailed insights in the functioning of the underlying biological system. For example, tracer kinetics combined with absolute protein concentrations have led to observations such as increased rates of the production of Aβ in carriers of the PSEN1 mutation and a reported dose-dependent decrease in Aβ production with γ-secretase inhibitors in humans[11,14]. The technique has also been applied to define a clear related change in slowed Aβ half-life and increasing age[12].

The objective of the current investigation is to compare the findings of the novel systems pharmacology model of the APP pathway to the tracer kinetic data. To this end, we extended the recently developed systems pharmacology model, by accounting for tracer dynamics throughout the APP pathway. Such an approach involves a quantitative analysis of the drug concentrations, plasma tracer enrichment and biomarker responses (absolute and fraction labelled proteins) using a comprehensive mathematical model that describes the underlying biological processes, while making a strict distinction between drug-specific and systems specific parameters. This allows for detailed interpretation of the biomarker responses by accounting for interdependencies among biomarkers as well as allowing for separation of rate *versus* extent of effects on the system. In this manner invaluable information is obtained on the functioning of the integrated biological system.

Dose ranging, biomarker, plasma tracer enrichment and pharmacokinetic data obtained from cisterna magna ported (CMP) rhesus monkeys receiving single doses of the BACE1 inhibitor MBi-5 and an infusion of the stable isotope tracer $^{13}C_6$-labelled Leucine ($^{13}C_6$-L) were available. The biomarkers measured were APP metabolites (Aβ40, Aβ42, sAPPβ and sAPPα); their concentrations were determined by ELISA. SILK was utilized to determine plasma enrichment $^{13}C_6$-L and fraction $^{13}C_6$-L labelled APP metabolites (fraction labeled sAPPβ, fraction labeled sAPPα, fraction labeled total Aβ).

The application of a systems pharmacology model based analysis accounting for tracer dynamics throughout the APP pathway revealed the similarities and differences in response measurements to BACE1 inhibition as determined by ELISA and SILK and these are discussed in this manuscript.

Materials and Methods

Animals

The CMP rhesus monkey model was described by Gilberto et al. (2003). The rhesus monkeys are chronically implanted with catheters in the cisterna magna, allowing repeated sampling of CSF and plasma. Six male animals, weighing between 5.2 and 11.7 kg (average, 8.7 kg), age 2 to 10 years (average, 8 years), were included in the study. Data from one animal was excluded from the analysis because of problems with the GS-MS.

These monkeys were captive-bred in a closed colony and individually housed. Animal use procedures were conform to the Guide for the Care and Use of Laboratory Animals[16].

In vivo labeling protocol

The $^{13}C_6$-Leucine infusion protocol was previously described by Cook et al. (2010). In brief, the monkeys were administered $^{13}C_6$-labelled Leucine ($^{13}C_6$-L) intravenously, with a primed infusion of 4 mg/kg bolus over 10 minutes, followed by 12 h of continuous infusion at a rate of 4 mg/kg/h. The primed 12 h $^{13}C_6$-L infusion was administered 1 hour post drug administration. The study protocol was described previously by Dobrowolska et al. (2014). CSF was sampled at -21, -19, 0 (pre-drug dose) and 3, 5, 7, 9, 13, 16, 19, 22, 25, 28, 31, 49, 55, 58, 73 and 145 h post drug administration, resulting in 19 samples for each monkey per treatment group to determine fraction labeled total Aβ, fraction labeled sAPPα and fraction labeled sAPPβ. Blood was sampled at 0 (pre-drug dose) and 3, 5, 7, 9, 13, 16, 19, 22, 25, 28, 31 and 49 h post drug administration resulting in 13 samples for each monkey per treatment group to assess the $^{13}C_6$-L enrichment in plasma.

GC-MS was used to quantify plasma $^{13}C_6$-L enrichment as previously described by Bateman et al. (2007) and Cook et al. (2010). $^{13}C_6$-L enrichment was quantified as a tracer-to-tracee ratio (TTR).

Aβ, sAPPα and sAPPβ were isolated by immunoprecipitation. To isolate Aβ a combination of the antibodies W0-2, directed against Aβ5-8, and HJ5.1, raised against Aβ13-28, was used. The proteins were proteolytically cleaved into smaller peptide fragments. LC-ESI-tandem MS was used to quantify the amount of $^{13}C_6$-L labeling in total Aβ, sAPPα and sAPPβ at each time point. Fraction $^{13}C_6$-L labelled protein was calculated as the fraction of the signal intensities for labelled peptide fragments over the sum of the signal intensities for labelled and unlabelled peptide fragments[17]. For Aβ, the peptide quantified was Aβ_{16-27}.

Drug administration and sampling

In a single dose, four-way, full crossover study, MBi-5 was administered at 10, 30, 125 mg/kg (5 mL/kg), or vehicle (0.4% methylcellulose) PO, with at least two weeks washout between each period. In conjunction $^{13}C_6$-L was administered as described above. Plasma and CSF drug concentrations were collected at 0 (pre-drug dose) and 3, 5, 7, 9, 13, 16, 19, 22, 25, 28, 31, 49, 55, 58, 73 and 145 h post-drug dose, resulting in 17 plasma and CSF PK samples for each monkey per treatment group. 2 mL of blood and 1 mL of CSF were collected at each time point. The concentration of MBi-5 in the plasma and CSF samples was determined using LC-MS/MS. The pharmacological profile of MBi-5 was summarized by Dobrowolska et al. (2014).

The concentrations of Aβ40, Aβ42, sAPPα and sAPPβ were collected at -22, -20 and -1 h (pre-drug dose) and 2, 4, 6, 8, 12, 15, 18, 21, 24, 27, 30, 48, 54, 57, 72 and 144 h post-drug dose, giving 19 measurements of each biomarker for each monkey per treatment. 1 mL of CSF were collected at each time point. The assays used for the protein concentration measurements were described previously[18,19,20]. Neoepitope-specific antibodies were used to detect Aβ40 and Aβ42, directed against Aβ1-40 and Aβ1-42.

PK-PD analysis

The PK-PD model has been developed and fitted to the data by means of non-linear mixed effects modelling using the NONMEM software package version 7 level 2[21]. The NONMEM software package was implemented on an Intel QuadCore (Intel® Core™ i7-3370 CPU, 3.40 GHz, 4.00 GB RAM) and Compaq Visual Fortran (version 6.6, Compaq Computer Corporation, Houston, Texas, USA) was used as compiler.

Modeling techniques were detailed by Van Maanen et al[9]. A decrease of 10.8 points in the minimum value of the objective function by adding an additional parameter, corresponding to $p<0.001$ in a χ-squared distribution, was considered significant. Data management and model assessment were done using the statistical software package S-PLUS for Windows (TIBCO Spotfire S+® 8.2, TIBCO Software Inc.).

To validate the model a visual predictive check (VPC) was performed in which the median and the 90% inter-quantile range of the data simulated with the developed model were plotted together with the observations. A validated result is close agreement of median observed and predicted line with $\sim$90% of the observations falling within the 90% prediction interval.

Model description

The systems pharmacology model of MBi-5 was based on sequential analysis of plasma tracer enrichment, PK and PD data. For the description of plasma enrichment over time a model that considers two pools for both $^{13}C_6$-L and $^{12}C_6$-L was developed (see Supplemental Material 1). The model related tracer input ($^{13}C_6$-Leucine infusion, in mg/kg/hr) to the measured enrichment (tracer to tracee ratio, TTR in%) in plasma. The PK model of MBi-5 was based on simultaneous analysis of plasma and CSF PK data (see van Maanen et al. (2016)). The PK profiles of MBi-5 observed in plasma and CSF were adequately described, thus the model could serve as input for PD model analysis.

The PKPD model accounting for labelled and unlabelled species is an extension of the model presented in van Maanen et al. (2016). For each individual monkey, the PK of MBi-5 and kinetics of plasma tracer enrichment were utilized as two independent inputs, by using individual parameter estimates of the respective kinetic models. The biomarker response profiles of MBi-5 measured in CSF were adequately described by a model containing expressions to describe the time courses of APP, sAPPβ, sAPPα, Aβ40, Aβ42, Aβ_O, FactorX (Fig. 4.1). sAPPβ, sAPPα, Aβ40 and Aβ42 were informed by data, whereas APP, Aβ_O and FactorX were inferred based on the model and the data of aforementioned biomarkers. FactorX represents other (unknown) analytes quantified in fraction labelled Aβ *(vide infra)*.

The production of APP was believed to be zero order, i.e. a constant production of APP. It was assumed that there is no alternative proteolytic enzyme cleaving full length APP other than α-secretase and BACE1. As both sAPPβ and C99 are products of APP cleavage by BACE1, sAPPβ and C99 were assumed to follow the same kinetics and therefore sAPPβ could be used in the model as surrogate precursor for Aβ. The production of sAPPα, sAPPβ and Aβ were assumed to be first order, i.e. dependent on the concentration of its precursor. To keep track of tracer dynamics throughout the pathway, two differential equations were implemented for each variable to account for labelled and unlabelled species, in which the tracer is assumed to be metabolically indistinguishable from the tracee. The system of differential equations is presented in Supplemental Material 4. The label incorporation in the APP pathway is driven by the kinetic model of plasma enrichment (Supplemental Material 4, Eq. S4.8 and S4.9). The inhibition of the BACE1 cleavage by MBi-5 was described by a sigmoidal Imax function (Supplemental Material 4, Eq. S4.22) using the individual predicted target site concentration of MBi-5, derived from the PK model (Supplemental Material 4, Eq. S4.23), as driver of the response.

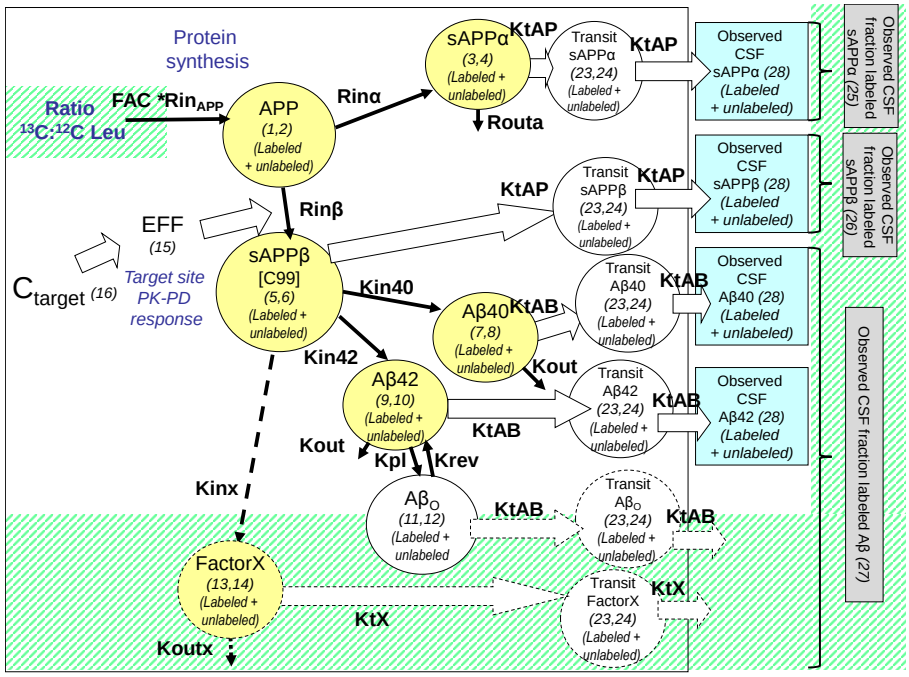

Figure 4.1: Schematic of systems model of APP processing.
The model comprised two times thirteen compartments: Six biomarker compartments in brain *(yellow circles)*, one oligomer compartment and six transit compartments from brain to CSF *(white circles)*, where each compartment was duplicated to track labelled and unlabelled species. Four biomarkers were measured in CSF (sAPPα, sAPPβ, Aβ40 and Aβ42), indicated by the blue boxes. Total concentrations (labelled plus unlabelled) of sAPPα, sAPPβ, Aβ40 and Aβ42 were measured using ELISA. Using SILK, fraction labelled sAPPα, fraction labelled sAPPβ and fraction labelled total Aβ were determined where fraction labelled total Aβ is labelled over total Aβ species. The drug effect *(EFF)* inhibited *Rin*β. C_{target}, derived from the PK model, was used as driver of the biomarker response in the model[9]. sAPPβ was used in the model structure as a surrogate substrate for C99 in the γ-secretase cleavage step. The tracer PK model of label enrichment of the Leucine pool (see Supplemental Material 1) informed label incorporation into the APP pathway.
Dashed arrows and compartments are additions to the model structure compared to the model based on ELISA data only[9]. Model extensions are indicated with the green shaded area. Equation numbers for each compartment have been included inside parentheses in order to facilitate their identification (see Supplemental Material 4).
APP: Aβ-precursor protein; *A*β: amyloid-β-peptide; C_{target}: drug concentration target site; Kin_{40}: Aβ40 formation rate; Kin_{42}: Aβ42 formation rate; Kin_{x}: FactorX formation rate; *Kout*: Aβ40 and Aβ42 degradation rate; *Koutx*: FactorX degradation rate; *Krev*: Oligomer dissociation rate; *KtAP*: transit rate sAPPα and sAPPβ from brain to CSF; *Kpl*: Oligomerization rate; *KtAB*: transit rate Aβ from brain to CSF; *RinAPP*: source of APP; *Rin*β: sAPPβ formation rate; *Rin*α: sAPPα formation rate; *Rout*: sAPPβ degradation rate; *Routa*: sAPPα degradation rate.

Results

Tracer enrichment in the brain

A kinetic model was used to describe the time course of the tracer enrichment in plasma during and after the infusion of the tracer. The model described tracer ($^{13}C_6$-L) and tracee (endogenous $^{12}C_6$-L) kinetics (see Supplemental Material 1).

Individual parameters from the kinetic tracer enrichment model were used to derive the enrichment at the target site in the brain. For this, the following assumptions were made: (1) there is no significant time delay between when the tracer is measured in plasma and when the tracer enters the brain. Any modest time delays in tracer entering the brain would be accounted for by later delay functions such as transit to CSF as the model could not independently assess this component of delay; (2) the shape of the enrichment-time profile in the brain is similar to that in plasma; (3) the probability of the incorporation of $^{13}C_6$-L into protein is the same as the probability that endogenous $^{12}C_6$-L is incorporated into protein; (4) none of the tracer incorporated into protein reappears as a consequence of protein breakdown in the time course of the tracer infusion. In the initial phase of tracer infusion the $^{13}C_6$-L incorporation in the APP metabolites is so small, that it is unlikely that $^{13}C_6$-L would be recycled by protein breakdown. Furthermore, protein turnover is assumed to be slow relative to the tracer infusion time.

No distinction can be made between the relative uptake of $^{13}C_6$-L in the APP pool and the transport of tracer from plasma to the brain. The blood-brain barrier transport is assumed not to be the rate-limiting step for $^{13}C_6$-L uptake in the APP pool. The relative formation of labelled and unlabelled APP species is related to the brain enrichment. Therefore, brain enrichment refers to the tracer ($^{13}C_6$-L) to tracee (endogenous $^{12}C_6$-L) ratio (TTR [%]) at the target site in the brain accessible for precursor (APP) formation. Consequently, brain enrichment can be derived using information from the placebo groups: if no inhibitor is given, and hence the system is in steady state, the sum of the labelled and unlabelled species is constant. A scale correction factor (*FAC*, see Supplement Material 4 Eq. S4.9) was applied to the plasma tracer enrichment, representing the relative uptake of tracer in the precursor (APP) pool. *FAC* was estimated to be 0.764 indicating that enrichment in the precursor pool was 76.4% of the level of plasma tracer enrichment.

Extension of the APP pathway model to account for tracer dynamics

Previously, a comprehensive systems model, incorporating the pharmacokinetics of MBi-5 and APP metabolites (Aβ40, Aβ42, sAPPα and sAPPβ) concentrations was developed[9].

The model quantified APP metabolite concentrations response to BACE1 inhibition and included an Aβ_{O} compartment that could account for the differential effect of MBi-5 on Aβ40 and Aβ42 response. sAPPβ was used in the model structure as a surrogate substrate for C99 in the γ-secretase cleavage step. As sAPPβ and C99 are both products of the same cleavage step, their formation rates should be the same. Modeling efforts to separately account for sAPPβ and C99 did not improve the model description of the data and, therefore, demonstrated adequacy of the surrogate assumption.

For the current analysis, this model was extended to account for tracer dynamics throughout the APP pathway (Figure 4.1). The $^{13}C_6$-L label incorporation into the APP pathway is determined from the derived brain tracer enrichment. To account for labelled and unlabelled species, two compartments were implemented for each variable (APP, sAPPβ, sAPPα, Aβ40, Aβ42, Aβ_{O}). Accordingly, the absolute amount of each APP metabolite is the sum of its labelled and unlabelled species and the fraction labelled APP metabolite is the ratio of labelled over the sum of its labelled and unlabelled species, with the exception of Aβ (Supplemental Material 4, Eq. S4.32-S4.34). In the SILK protocol no distinction was made between Aβ40 and Aβ42. Therefore, fraction labelled Aβ was initially assumed to be equal to the fraction labelled of total Aβ40 and Aβ42.

At first, the model structure and parameter values were fixed to those identified recently on absolute APP metabolite concentration data[9]. The model was then used to predict the fraction labelled proteins (SILK). Here, underprediction was observed for fraction labeled sAPPβ (placebo, dose 30 and dose 125 mg/kg, Fig. 4.4C, 4.4O, 4.4U) and fraction labeled sAPPα (placebo, 10 mg/kg, 30 mg/kg, Fig. 4.4A, 4.4G, 4.4M). Overprediction was observed for fraction labeled Aβ for all dose groups (Fig. 4.4E, 4.4K, 4.4Q, 4.4W). As the response measurements to BACE1 inhibition by ELISA and SILK were the result of inhibiting the same pathway step, difference in effects of BACE1 inhibition on the biomarkers was not expected. Therefore, the flawed model fit indicated that there was additional information content to be gained from the SILK data beyond that from the ELISA. As such this additional data helped to better refine the true mechanistic representation of the APP system.

Accounting for differences in APP metabolite response measurements by ELISA and SILK

Integrating kinetic modelling of labelled and absolute data allows for the inconsistency of the results to be more robustly evaluated beyond comparison of observed response measurements. The results indicated a inconsistency between response magnitudes by

ELISA and SILK within the framework of the previously established kinetic model. Likely, aspects misspecified would be related to how the label is incorporated into the pathway or in how the two quantitative measures related to each other.

It was hypothesized that differences in APP metabolite responses as measured by ELISA and SILK may be caused by some deeper compartment in the APP pathway that could not be identified based on ELISA data only. This could be an additional APP pool causing a release of labelled APP that feeds slowly into the system, or an C99 pool that gives a slow release of labelled C99 that feeds into the system. Inclusion of the additional APP pool in the model worsened the description of fraction labeled sAPPα (results not shown). This indicated that the cause of the discrepancy in measurements should be sought further down the APP pathway. It was not possible to identify an C99 model component based on the current dataset, with which it was not feasible to separate the γ-secretase cleavage step from sAPPβ elimination[9].

An understanding of the assay differences between SILK and ELISA could suggest another alternate explanation of the disconnect, as one technique may have measured analytes which the other did not. Possibilities include ELISA cross-reactivity to species which were not measured by the SILK method, e.g. η-secretase products[8], or SILK measured alternative APP fragments in addition to sAPPα, sAPPβ, Aβ40 or Aβ42. If the same analytes were measured in both methods, then fraction labeled Aβ (SILK) would be composed of labelled over total Aβ40 and Aβ42 species and absolute Aβ40 and Aβ42 protein concentrations (ELISA) would be the sum of its labelled and unlabelled species. If the analytes as measured in SILK differ from those in ELISA this assumption will not hold. Fraction labelled Aβ (SILK) is then composed of labelled over total Aβ40, Aβ42 and other analytes. Absolute Aβ40 and Aβ42 protein concentrations (ELISA) remain the sum of their labelled and unlabelled species. To address this, a FactorX compartment was incorporated in the model representing these other analytes.

It was investigated if the other analytes represented by FactorX have a similar degradation rate (*Koutx*) as Aβ40 and Aβ42 (*Kout*). The formation rate of FactorX (*Kinx*) was defined by steady state conditions and derived from the other parameters (Supplement Material 4 Eq. S4.29). As a result, *Kinx* had a different value than *Kin40* and *Kin42*. With the similar degradation rate and the derived formation rate of FactorX, the inclusion of FactorX in the calculation of fraction labeled Aβ had no impact on the fraction labeled Aβ curve (not shown). Because mathematically terms were canceled out in the calculation of fraction labeled Aβ including FactorX, the same fraction labeled Aβ as

based on only labelled over total Aβ40 and Aβ42 species was obtained. This indicated

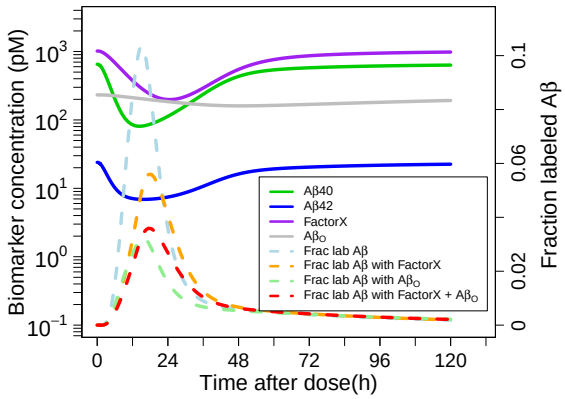

Figure 4.2: Graphical insight into the Aβ biomarker responses in CSF, using the identified systems model of the APP processing pathway.
The biomarker responses in CSF are predicted after a single dose of 125 mg MBi-5, using the typical parameter estimates.
Aβ40 green solid line; *Aβ42* blue solid line; *FactorX* purple solid line; *Aβ_O* grey solid line; *fraction labeled Aβ* light blue dashed line; *fraction labeled Aβ with FactorX* orange dashed line; *fraction labeled Aβ with Aβ_O* light green dashed line; *fraction labeled Aβ with FactorX and Aβ_O* red dashed line.

that the analytes that were hypothesized to be additionally measured in SILK had to have different kinetics. Therefore, a different degradation rate for the analytes represented by FactorX was included in the model. The transit rate from brain-to-CSF for FactorX (*KtX*) was assumed to be similar to the transit rate for Aβ species (Aβ40 and Aβ42). The model including FactorX labelled and unlabelled species, with different kinetics for FactorX than for Aβ40 and Aβ42, improved the description of the SILK data (results not shown). Description was further improved by also including labelled over total Aβ_O in fraction labelled Aβ as determined in CSF. For this, the transit of Aβ_O from brain to CSF needed to be added to the model structure. This facilitated the identification of the Aβ_O transit rate. When estimated the Aβ_O transit rate was similar to the Aβ transit rate from brain to CSF (*KtAB*) and could therefore be fixed to the same high value ($10\,h^{-1}$)[9]. It was not possible to identify the brain-turnover of Aβ_O as a separate parameter. Therefore, the Aβ_O half-life of 0.07 h reflects delays due to the brain-turnover and brain-to-CSF transfer. The value of the transit rate for sAPPα and sAPPβ *(KtAPP)* should be interpreted relative to the Aβ transit rate. By fixing *KtAB* all possible delay is lumped in *KtAPP*.

The right panels in Fig. 4.4 show the description of the SILK data for the model with FactorX and Aβ_O included in the calculation of fraction labelled Aβ. A prediction was performed with the model to investigate the contribution of FactorX and Aβ_O to

the fraction labeled Aβ curve (Fig. 4.2). The FactorX level was slightly higher than Aβ40 and the shape of the FactorX response curve was different from the Aβ40 and Aβ42 responses due to the different degradation rate of FactorX (*Koutx*). Inclusion of FactorX and Aβ_{O} in fraction labeled Aβ had a lowering effect on the fraction labelled Aβ curve and slightly altered its shape.

Comparison results based on ELISA and SILK *versus* ELISA only

Administration of MBi-5 increased sAPPα and decreased sAPPβ, Aβ40 and Aβ42 concentrations in a concentration driven saturable effect as measured by ELISA (Fig. 4.5). A concentration-dependent response was also identified for the fraction labeled profiles of Aβ and sAPPβ. For the fraction labeled profile of sAPPα, the drug effect was almost absent (Fig. 4.4). One single drug effect could describe the concentration-dependent response of all biomarkers, including the lack of response for fraction labeled sAPPα.

Predictions from the systems model (Fig. 4.3) show that BACE1 inhibition resulted in a MBi-5 concentration driven accumulation of APP, leading to an increased production of sAPPα as APP is shunted down the α-secretase pathway. Both labelled and unlabelled species accumulate in a dose-dependent manner as result of BACE1 inhibition, but as the tracer infusion starts one hour post drug administration, the relatively more unlabelled species than labelled species accumulate. Due to the fractional nature of the fraction labeled measurement, these unlabelled species dilute the apparent response, from the start of drug treatment. Therefore, although there is a MBi-5 concentration driven increase in APP, this is not reflected in the 'fraction labeled APP' curve. The fraction labelled sAPPα is dependent on labelled APP and dilution by the accumulation of unlabelled sAPPα. Consequently, minimal drug concentration-dependent increase appeared from the fraction labelled sAPPα curve, even though there is drug concentration driven increase in sAPPα formation. The same effect does not occur for fraction labeled sAPPβ. The labeling process is continuous during the tracer infusion and washout, as is the APP accumulation during BACE1 inhibition. However, during the one hour time period between drug administration and start of tracer infusion there is no accumulation of unlabelled sAPPβ, as sAPPβ levels are reducing as result of BACE1 inhibition. Therefore, there is no dilution of the apparent fraction labeled sAPPβ response by unlabelled sAPPβ species.

The drug potency (IC_{50}) identified in the combined analysis of ELISA and SILK data was 0.0267 μM (95% CI, 0.0201-0.0333), comparable to the IC_{50} identified on ELISA data only (0.0269 μM (95% CI, 0.0154-0.0384))[9]. This value is also close to the *in vitro* inhibition constant (Ki) of 10 nM for MBI-5 inhibition of purified BACE1[17]. The Hill

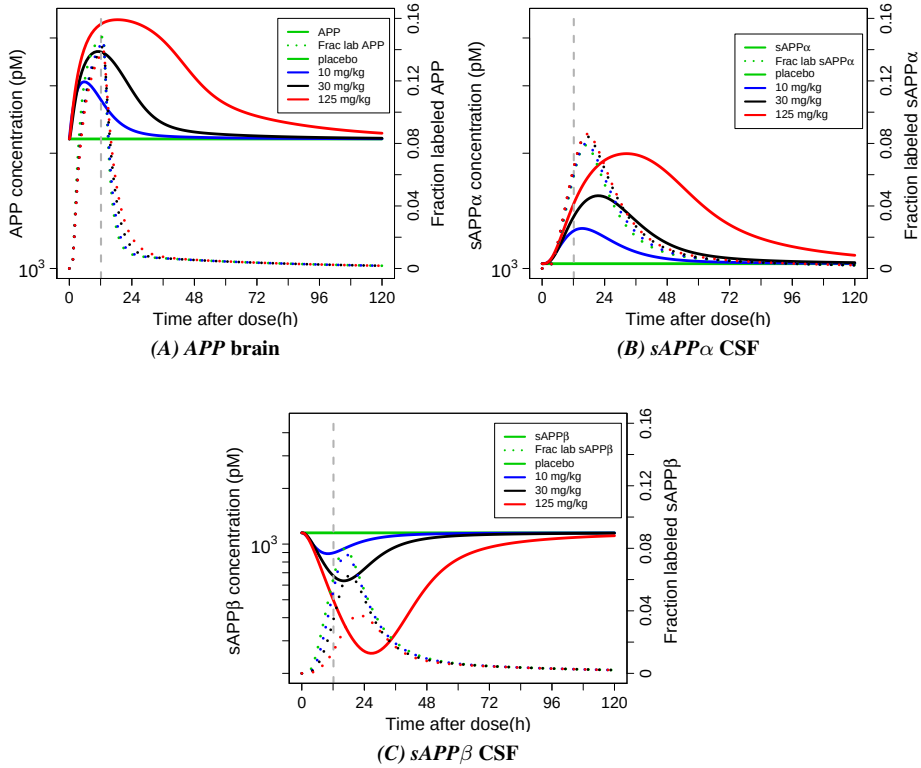

Figure 4.3: Predicted APP in brain* (A)*, sAPPα in CSF* (B) *and sAPPβ in CSF* (C) *responses, using the identified systems model of APP processing.
The biomarker responses are predicted after a dose range of MBi-5, using typical parameter estimates.
Absolute protein concentrations: solid line; *Fraction labelled proteins:* dotted line; *Placebo:* green; *Dose 10 mg/kg:* blue; *Dose 30 mg/kg:* black; *Dose 125 mg/kg:* red; *End time of tracer infusion:* vertical grey line.

coefficient of the concentration response relationship significantly changed from 1.53 (95% CI, 1.44-1.92) based on ELISA data to 0.986 (95% CI, 0.963-1.01) based on ELISA and SILK data. As the Hill coefficient was not significantly different from 1, the sigmoid-emax concentration response relationship could be reduced to an Emax relationship by fixing the Hill coefficient to 1. A Hill coefficient of 1 is the theoretical value for a simple receptor-target interaction. The shift to this value based on the ELISA and SILK data suggested that a more distinct representation of the inhibitor interaction with the target was achieved.

The Hill coefficient of unity based on ELISA and SILK data indicated a less steep

concentration response relationship than was identified on ELISA data only. Based on the ELISA and SILK data, inhibition rises much less quickly with concentration than expected based on the recent result. This mainly affected the description of the APP metabolite concentration response curves for the higher dose groups (Fig. 4.5)[9].

The brain-turnover of sAPPα was slower based on the combined analysis (1.6 h) compared to based on ELISA data only (0.8 h). The identified proteolytic cleavage rates of APP by BACE1 and α-secretase imply that 49.1% of endogenous full length APP is cleaved by BACE1 and 50.9% by alternate pathways represented by the terms for α-secretase. These results are similar to the percentages APP identified to go down each path based on ELISA data only (44% and 56%, respectively)[9].

A sequence of models with interanimal variability on different parameters was tested and the results compared, in order to select the best random effects model structure. The final model included interanimal variability on the baseline level of sAPPβ and FAC. The identified interanimal variability on the baseline level of sAPPβ also reflects on the baseline levels of the other APP metabolites, because of their interrelationships. Interanimal variability could not be identified for the drug effect parameters, indicating that the variation in drug effect was small relative to the underlying biologic variation in the system. Residual variability for absolute protein concentrations were implemented as proportional error models. Residual variability was higher for Aβ40 and Aβ42 than for sAPPβ and sAPPα. Residual variability for fraction labelled proteins was implemented as an additive error model.

Table 4.1: Population parameter estimates including coefficient of variation (CV%) for updated model based on ELISA and SILK data.

PARAMETER	DESCRIPTION	VALUE	UNIT	CV%
Structural parameters				
sAPPβ_{base}	baseline sAPPβ	1.15e+003	pM	6.23
Fbase$_{\mathrm{A}\beta 40}$	Aβ40 baseline as fraction of sAPPβ_{base}	0.566		7.83
Fbase$_{\mathrm{A}\beta 42}$	Aβ42 baseline as fraction of sAPPβ_{base}	0.0208		5.58
Fbase$_{\mathrm{sAPP}\alpha}$	sAPPα baseline as fraction of sAPPβ_{base}	0.895		2.20
Fbase$_{\mathrm{X}}$	FactorX baseline as fraction of sAPPβ_{base}	0.883		26.6
Rout$_{\mathrm{a}}$	degradation rate sAPPα	0.427	h^{-1}	5.53
Kout	degradation rate Aβ40 and Aβ42	0.603	h^{-1}	7.05
Kout$_{\mathrm{x}}$	degradation rate FactorX	0.138	h^{-1}	9.78
KtAP	transit rate sAPPα and sAPPβ	0.110	h^{-1}	5.04
KtAB[a]	transit rate Aβ	10	h^{-1}	
FAC	scale correction factor	0.764		2.50
Kpl	oligomerization rate	0.164	h^{-1}	42.0
Krev	oligomer dissociation rate	0.0169	h^{-1}	35.4
IM[a]	Imax	1		
IC50	IC50	0.0267	μM	12.5
Interanimal variability				
$\omega^2{}_{\mathrm{BSAPb}}$ [b]	Interanimal variability sAPPβ baseline	0.0670		22.5
$\omega^2{}_{\mathrm{FAC}}$ [b]	Interanimal variability scale correction factor (FAC)	0.0127		44.7
Residual error				
$\sigma^2{}_{\mathrm{A}\beta 40}$ [c]	Residual variability Aβ40	0.266		15.4
$\sigma^2{}_{\mathrm{A}\beta 42}$ [c]	Residual variability Aβ42	0.126		10.6
$\sigma^2{}_{\mathrm{sAPP}\beta}$ [c]	Residual variability sAPPβ	0.0548		14.6
$\sigma^2{}_{\mathrm{sAPP}\alpha}$ [c]	Residual variability sAPPα	0.0625		8.19
$\sigma^2{}_{\mathrm{FracLab}}$ [c]	Residual variability fraction labelled	4.62e-005		7.40

[a] Fixed.
[b] Interanimal variability is assumed to follow a normal distribution with mean zero and variance ω^2.
[c] Residual variability is assumed to follow a normal distribution with mean zero and variance σ^2.

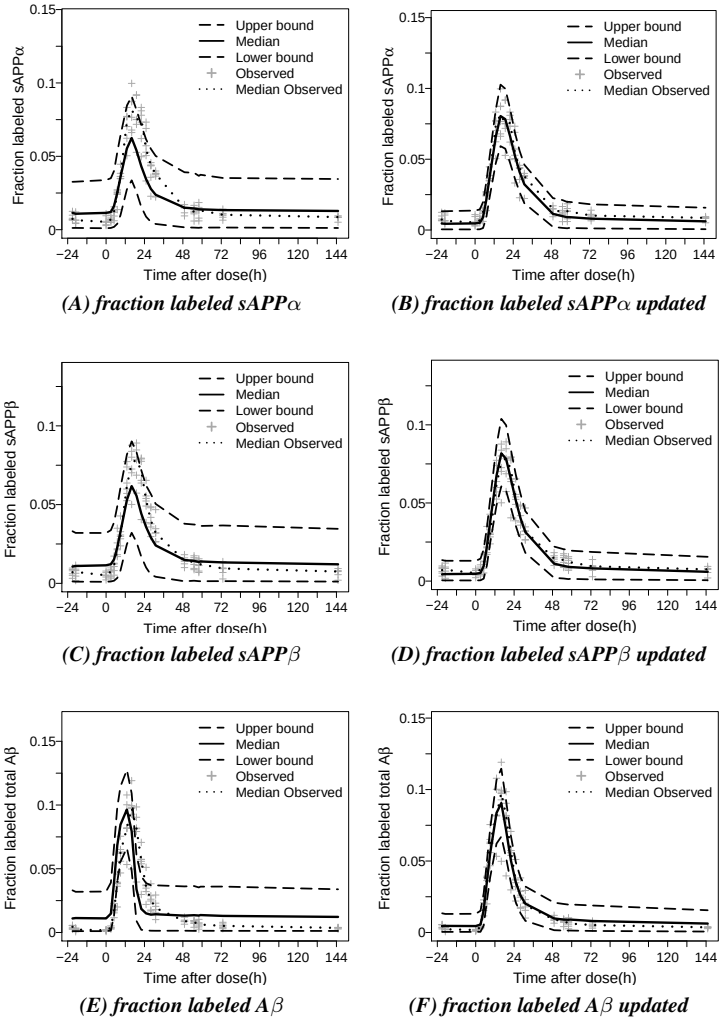

(A) fraction labeled sAPPα ***(B) fraction labeled sAPPα updated***

(C) fraction labeled sAPPβ ***(D) fraction labeled sAPPβ updated***

(E) fraction labeled Aβ ***(F) fraction labeled Aβ updated***

Figure 4.4: Visual predictive check of fraction labeled protein response* vs. *time profile of MBi-5 in the rhesus with 90% confidence interval.

Predictions were performed with model based on ELISA data only (*left*) and updated model based on ELISA and SILK data (*right*). Placebo (*A-F*), dose 10 mg/kg (*G-L*), dose 30 mg/kg (*M-R*) and dose 125 mg/kg (*S-X*). Observation sample size: n=95 for each SILK biomarker from 5 monkeys collected over 7 days at 4 occasions.

Solid line: Median model predicted fraction labeled protein response-time profile; *Long-dashed line:* 90 % prediction interval; *Dotted line:* Median observed fraction labeled protein response-time profile; + *symbol:* Observations.

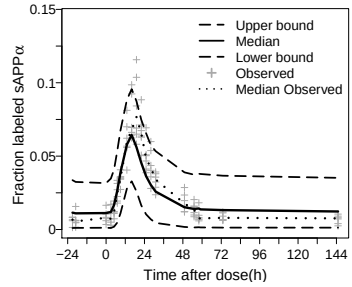

(G) fraction labeled sAPPα

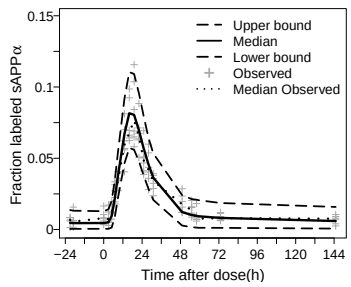

(H) fraction labeled sAPPα updated

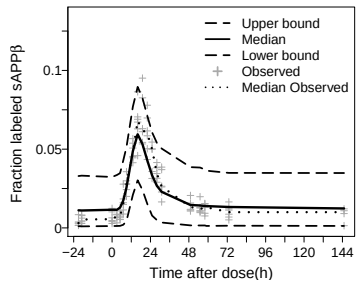

(I) fraction labeled sAPPβ

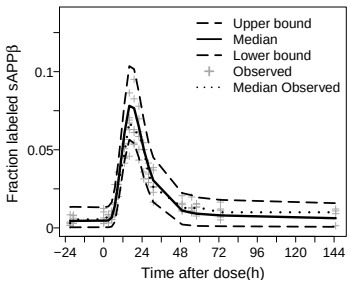

(J) fraction labeled sAPPβ updated

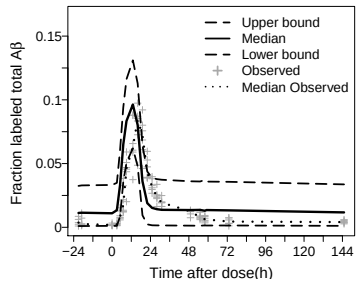

(K) fraction labeled Aβ

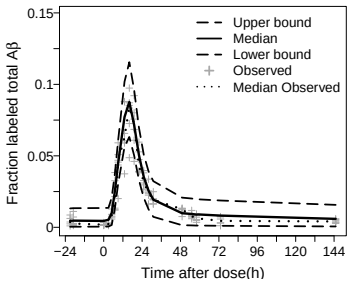

(L) fraction labeled Aβ updated

Figure 4.4: (Continued)

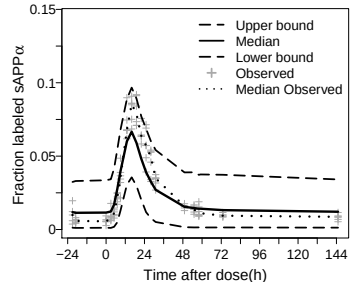

(M) fraction labeled sAPPα

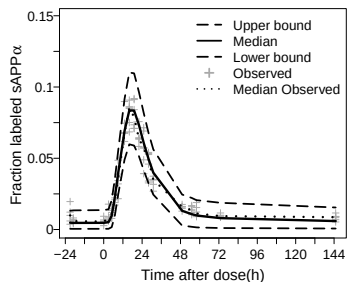

(N) fraction labeled sAPPα updated

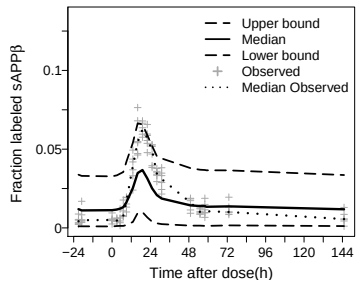

(O) fraction labeled sAPPβ

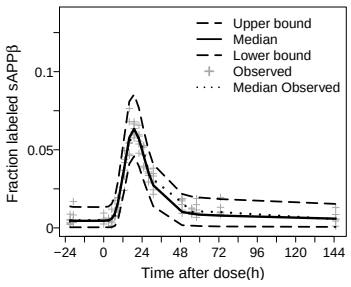

(P) fraction labeled sAPPβ updated

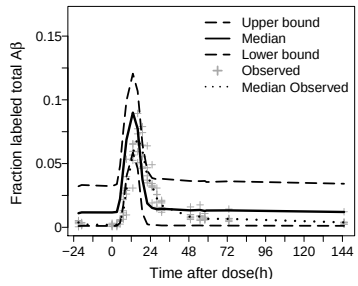

(Q) fraction labeled Aβ

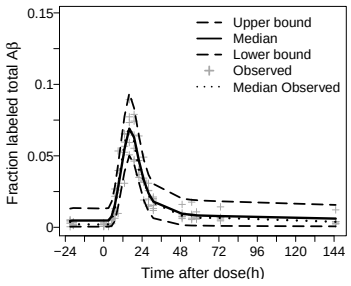

(R) fraction labeled Aβ updated

Figure 4.4: (Continued)

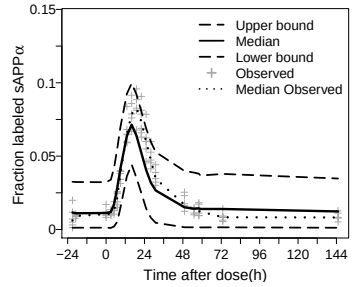

(S) fraction labeled sAPPα

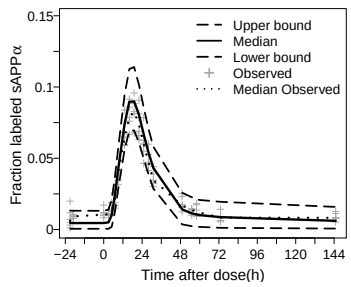

(T) fraction labeled sAPPα updated

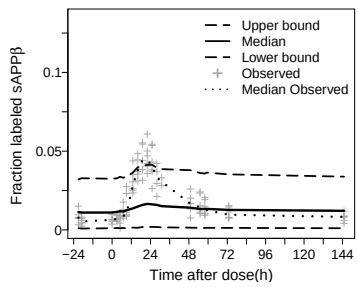

(U) fraction labeled sAPPβ

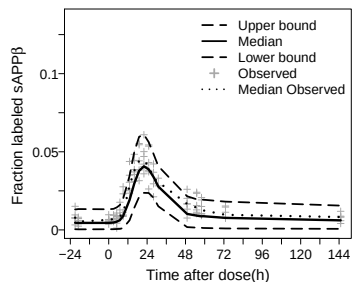

(V) fraction labeled sAPPβ updated

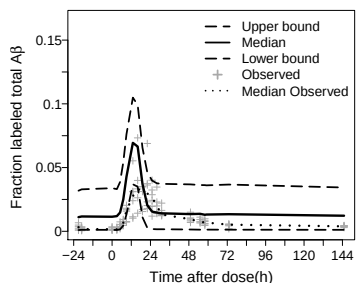

(W) fraction labeled Aβ

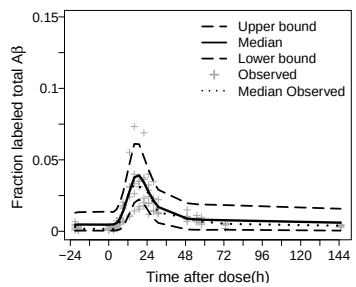

(X) fraction labeled Aβ updated

Figure 4.4: (Continued)

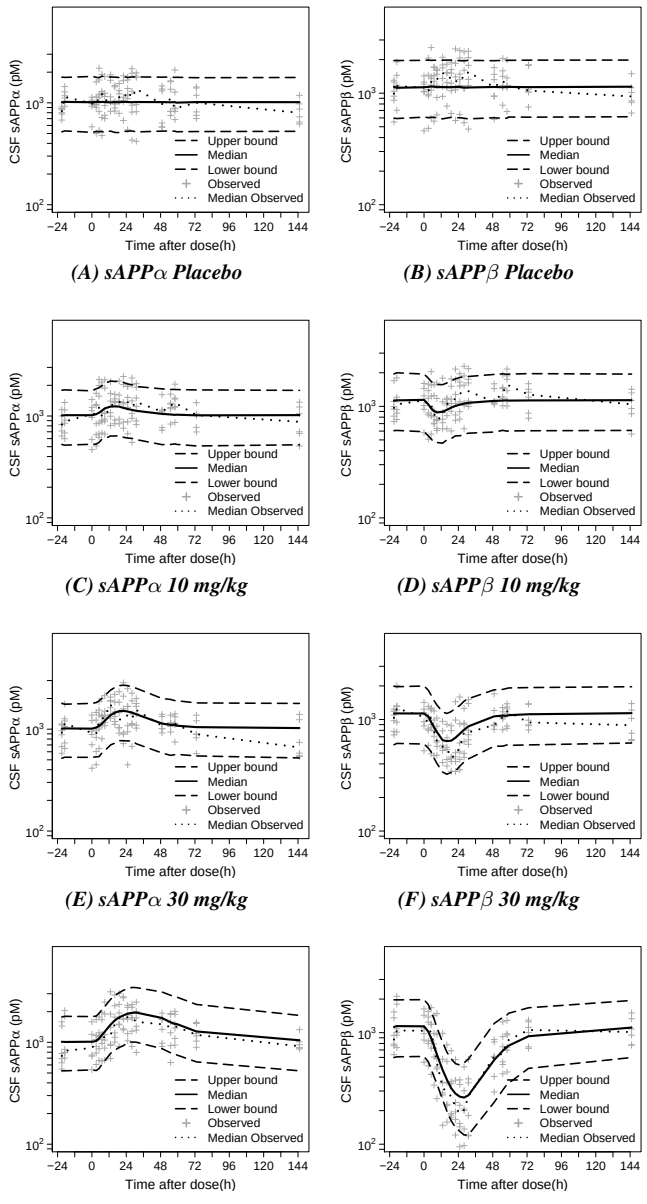

Figure 4.5: Visual predictive check of sAPPα (**left: A,C,E,G*****), sAPPβ (*****right: B,D,F,H*****), Aβ40 (*****left: I,K,M,O*****) and Aβ42 (*****right: J,L,N,P*****) concentration response vs. time profile of MBi-5 in the rhesus with 90% confidence interval.*** Predictions were performed with updated model based on ELISA and SILK. Observation sample size: n=95 for each APP metabolite from 5 monkeys collected over 7 days at 4 occasions. *Solid line:* Median model predicted concentration-time profile *Long-dashed line:* 90 % prediction interval. *Dotted line:* Median observed concentration-time profile + *symbol:* Observations.

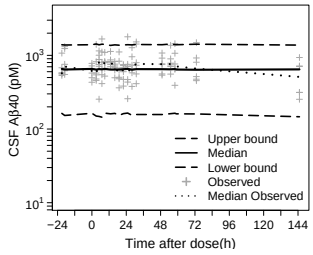

(I) Aβ40 Placebo

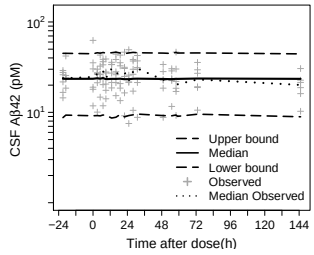

(J) Aβ42 Placebo

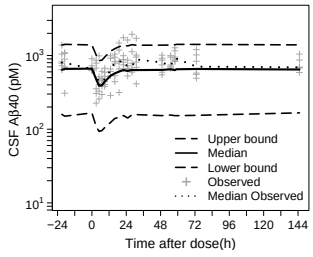

(K) Aβ40 10 mg/kg

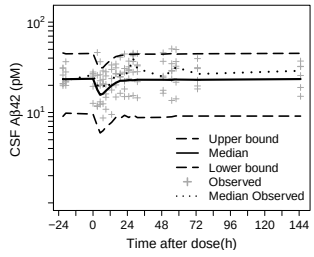

(L) Aβ42 10 mg/kg

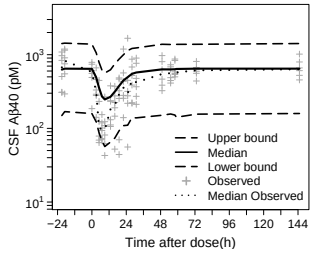

(M) Aβ40 30 mg/kg

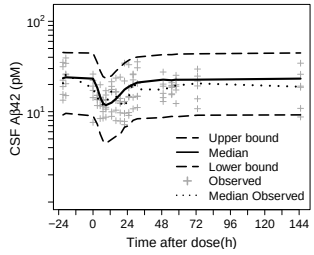

(N) Aβ42 30 mg/kg

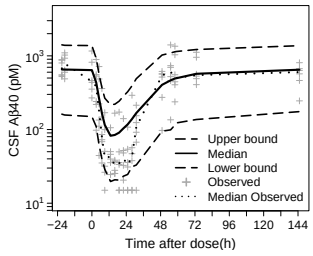

(O) Aβ40 125 mg/kg

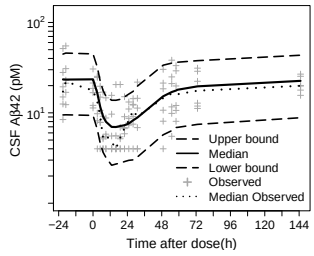

(P) Aβ42 125 mg/kg

Figure 4.5: (Continued)

Discussion

Tracer kinetic studies are widely used to determine the influence of enzyme inducers or inhibitors on the rates of production and degradation of proteins. Traditionally, a non-compartmental analysis of the tracer enrichments versus time curve is used to estimate their effects on the rates of protein production and/or degradation. The rate of protein production being estimated from the upswing of the curve and the rate of degradation from the downswing. It has been demonstrated that the use of non-compartmental tracer kinetic data analysis where the enrichment is not in steady state could lead to inaccurate quantification of kinetic parameters [22].

Alternatively, compartmental models have been used for this purpose [23,24]. Here typically a standard two stage is followed in which each individuals PD parameters are estimated and then population mean and variance of each parameter are derived[25]. A limitation of this approach is that the effect on protein disposition is related to the dose rather than to measures of drug concentrations.

To our knowledge, we are the first to utilize a population PK-PD modelling approach to the analysis of tracer kinetic data. The approach utilized here, in which the time course of the plasma tracer enrichment is analysed in conjunction with the time course of the plasma and CSF concentrations of the BACE1 inhibitor MBi-5, is novel for this type of data. The individual values of the (pharmaco)kinetic parameters obtained in these models serve as input for the modelling of the time course of the tracer enrichment of the APP metabolites. This enabled characterization of the concentration-enrichment-effect relationship of the BACE1 inhibitor, while taking into account the variability in PK, enrichment and PD in the study population.

We have recently been able to propose a systems pharmacology model for the APP processing pathway based on absolute concentrations of APP metabolites in rhesus monkeys[9]. This model provided a unique opportunity to further evaluate our understanding of the APP processing pathway while including tracer kinetic data in addition to absolute protein measurements. To this end we have simultaneously analysed the effects of a BACE1 inhibitor on the APP processing pathway, by analyzing the effects on tracer kinetic parameters (fraction labelled of various peptide species) as well as absolute protein concentrations. This has yielded invaluable information on the nature of measurements used in both techniques and on the underlying physiology.

The application of the existing systems pharmacology model to the combined dataset was generally consistent with our understanding of the APP processing pathway and

the existence of the oligomer pool. Moreover, the parameters describing the formation and degradation of the APP metabolites were comparable thereby strengthening our understanding of the relative contribution of the different analytes to the observed responses.

In the presence of the BACE1 inhibitor MBi-5 a concentration dependent saturable decrease in Aβ40, Aβ42 and sAPPβ concentrations was observed in combination with an increase in sAPPα absolute protein concentrations. In the SILK assay fraction labelled profiles for Aβ and sAPPβ were reduced in a similar MBi-5 concentration-dependent manner. However, the effect on the fraction labelled profile of sAPPα was negligible. This is explained by the fact that the effect on sAPPα is an indirect effect through the accumulation of APP, secondary to the inhibition of BACE1. As the concentrations of both unlabelled and labelled sAPPα change in the same direction, there is no clear effect on the ratio labelled over total sAPPα (= the fraction labelled). This is further augmented by the fact that the tracer infusion starts one hour after MBi-5 administration. In this first hour after the administration of the BACE1 inhibitor unlabelled sAPPα starts to accumulate while there is no accumulation of labelled sAPPα. This further dampens the effect on the fraction labelled sAPPα. Finally, after a single dose of the BACE1 inhibitor, the observed dose response relationship also depends on the end time of the tracer infusion relative to the time of the maximal PD response.

In contrast to the attenuated effects of BACE1 inhibition on parameters characterizing the α-secretase pathway (fraction labelled sAPPα), clear effects on the parameters of BACE1 pathway (fraction labelled sAPPβ, fraction labelled Aβ) were observed, which is explained by the fact that these parameters are all downstream of BACE1, so that there is no accumulation of unlabelled protein in the time between drug administration and start of tracer infusion. These observations show, that due the complexity of the underlying biochemical network, lack of concentration dependent effect of an enzyme inhibitor on certain parameters, does not exclude the possibility that there is indeed such an effect.

We found a lower brain tracer enrichment relative to plasma tracer enrichment during $^{13}C_6$-L infusion (Supplemental Material 3, Figure S4.4). The discrepancy between plasma tracer enrichment and target site enrichment may be explained by a lower amount of tracer at the target site, due to dilution of tracer. This may be the result of a higher amount of endogenous Leucine at the target site than in plasma. Also, kinetics of Leucine into and out of the cells, as well as into and out of the corresponding protein pools can differ across tissues [22].

The lower relative enrichment at the target site indicates that $^{13}C_6$-L does not achieve

an isotopic equilibrium throughout all free pools of Leucine in the time frame of tracer infusion. This is also observed in the plasma tracer enrichment data, where plasma TTR is still rising during the 12 h infusion. This was confirmed by simulations using the developed model, indicating that it takes approximately 52 days of infusion to reach steady state with the primed-constant infusion technique as used in SILK (see Supplemental Material 1, Figure S4.3). With the primed 12 h infusion used in the current study, 62% of the steady state level of plasma tracer enrichment was reached. Therefore, the plateau observed in plasma tracer enrichment is a pseudo steady-state. The absence of steady state in tracer enrichment requires an analysis which takes into account the dynamics of the system, such as a comprehensive model based analysis performed currently.

The extension of the systems pharmacology model to include tracer kinetic data provides additional insights into the underlying APP processing pathway. Our modelling results indicate that 49.1% of APP is cleaved by BACE1 and 50.9% by α-secretase. It was assumed that all alternate pathways were represented by the terms for α-secretase. The reported percentage of APP to go down the α-secretase path should be interpreted as capturing the contribution of alternate pathways in general, as it acts to mediate the increase in APP which drives the α-secretase response and any other alternate pathway response. Increases in APP due to BACE1 inhibition result in more substrate being available to alternate pathways in general and α-secretase as an alternate path well represents this phenomena. It is expected that all alternate paths will behave dynamically as α-secretase does as all drug effects on alternate paths will be driven by the APP increase under BACE1 inhibition. The increases seen with α-secretase and captured in this model should also reflect the relative changes to be expected for any alternate pathway that may be present. Therefore, it is expected that sAPP-η would build-up in response to BACE1 inhibition similar to sAPPα build-up. An accumulation of the cleavage products of η-secretase after BACE1 inhibition was also reported by Willem et al 2015 in mice.

The simultaneous analysis of the combined data revealed differences in Aβresponses after BACE1 inhibition in rhesus monkeys as determined by ELISA and SILK. In a model-based analysis, in which knowledge of the biological system and analytical methods was integrated, various hypotheses to align APP metabolite response measurements in ELISA and SILK were tested. A possible explanation of the disconnect may be that an unknown process or analytes other than Aβ40 (Aβ1-40) and Aβ42 (Aβ1-42) were measured in SILK and not ELISA. The incorporation of the FactorX compartment in the model accounted for this (Fig. 4.1). The disconnect in measurements between both methods may be explained by the use of different measurement techniques. The antibodies

used in the ELISA where neoepitope-specific antibodies (N-terminal antibodies), directed against Aβ1-40 and Aβ1-42. The antibodies used to isolate Aβ in the SILK protocol were not end-specific for the N- or C-terminus, but directed against Aβ5-27. As the antibodies used to isolate Aβ were raised against Aβ5-27, these analytes that were detected in this assay must include this amino acid sequence.

A new APP processing pathway was recently reported by Willem et al 2015, in which sequential cleavage of APP by η-secretase and BACE1 or ADAM10 leads to the formation of Aη-β and Aη-α, respectively. Several Aη peptides were reported by Willem et al 2015, that could have been captured by antibody W0-2, but not by HJ5.1, as used in the SILK protocol. Therefore, this does not explain the disconnect.

In an alternative path, BACE1 can cleave full length APP at the β-prime site (GLU11 in the Aβ sequence) leading to the production of Aβ11-40 and Aβ11-42. These are major cleavage products of BACE1, as reported by[26]. Both Aβ11-40 and Aβ11-42 could not have been captured by the antibody W0-2 used in the SILK protocol, nor the neoepitope-specific antibodies used in the ELISA. Thus, β-prime site cleavage products cannot explain a difference in measurements between both methods.

It could be that ELISA does not detect the full complement of Aβ42, as it is either tied up in Aβ_{O} or bound to a carrier protein[27]. The methods used to detect the fraction labelled Aβ in the SILK protocol should also capture Aβ_{O}. How rapidly newly synthesized Aβ becomes an oligomeric species and how rapidly Aβ_{O} would move from brain to CSF is not known, but they are likely cleared to CSF much more slowly than the monomer due to their biophysical properties. It could also be that there is active transport of soluble toxic Aβ_{O} out of the brain, resulting in faster brain-to-CSF transport than for monomeric species. It was not possible to identify the brain-turnover of Aβ_{O} and turnover over brain-to-CSF transport as separate parameters. Therefore, the half-life of Aβ_{O} of 0.07 h reflects delays due to both brain-to-CSF transfer and turnover in the brain. Therefore, the rate of appearance of Aβ_{O} response in CSF relative to Aβ cannot be appointed to one of these processes.

Remarkably, different kinetics were identified for the process or analytes represented by FactorX, compared to Aβ40 and Aβ42. It was not possible to separate the rate of the γ-secretasecleavage from the brain-to-CSF transport. Therefore, the transit rates from brain-to-CSF for Aβ40, Aβ42 (KtAB) and FactorX (KtX) were fixed to an arbitrary high value (10 h-1) and assumed to be equal.

Consequently, the Aβ40 and Aβ42 half-life of 1.1 h reflects delays due to the γ-secretase cleavage step and brain-to-CSF transfer. The current model structure in which

Aβ40 and Aβ42 are directly formed is a simplification of the underlying system. γ-secretase cleaves C99 through interactive pathways for stepwise successive processing to generate different Aβ isoforms, with Aβ40 and Aβ42 as the major products[28]. The initial γ-secretase cleavages are followed sequentially by γ-secretase cleavages after every three or four residues. The systems model was able to combine two types of data and describe seven biomarkers successfully. Adding the tracer kinetic data (SILK) to the model based on absolute protein concentrations (ELISA)[9] confirmed the system that was identified on ELISA data only. This is one utility of the biomarkers of the SILK protocol. Our understanding of the relationships among the absolute APP metabolite concentrations did not change compared to the recent analysis based on ELISA data only. However, the combined analysis allowed for more hypotheses to be tested. Vice versa, including absolute protein concentrations in the interpretation of the tracer kinetic data had added value. This facilitated the correct interpretation of drug concentration dependencies in the tracer kinetic data and led to the investigation of a disconnect in the two type of measurements of the same system, which was accounted for by the FactorX model component.

If dedicated measurements of Aβ1-40 and Aβ1-42 were used in the SILK protocol, it is expected that Aβ40, Aβ42, fraction labelled Aβ could have been described by a model without inclusion of the FactorX model component. However, even then, matrix components in the CSF may affect the measurement reproducibility across different immunoassays[27].

In a follow-up study, dedicated measures of Aβ40, Aβ42 and Aβ38 will be performed in the same samples in both labelled and absolute quantification. In addition, Aβ will be quantified using an antibody directed at the mid-domain Aβ17-28. If FactorX is an Aβ isoform, it would then be possible to determine if it has different half-lifes from Aβ40, Aβ42 and Aβ38 and how much FactorX accounts for total of Aβ species compared to Aβ40, Aβ42 and Aβ38.

Conclusion

This investigation demonstrated that the simultaneous analysis of absolute protein concentrations and tracer kinetic data using a systems pharmacology model will elucidate the underlying biological system and will thereby facilitate the interpretation of the tracer kinetic data in the light of the system. The model-based analysis distinguished labelled and unlabelled species, as well as separated steps in the APP pathway and distribution to CSF. This enabled and improved understanding of the (lack-of) dose-dependent response in kinetic data.

Different hypotheses to align APP metabolite response measurements in ELISA and SILK were tested. A possible explanation of the disconnect may be that an unknown APP fragment with differing kinetics or an unknown process was picked up in SILK assay. This requires further investigation.

The developed comprehensive model can be used to perform simulations to investigate study design features that may influence the magnitude of biomarker responses, such as dose and degree of Aβ production inhibition. To maximize information on the APP pathway from the tracer protocol, simulations can be performed to investigate how the $^{13}C_6$-L infusion time and length affects the fraction labelled curves (ongoing). It is anticipated that adding information on APP metabolite responses (absolute and fraction labelled proteins) following γ-secretase inhibition will provide more information on the biological system as well as the discrepancies between absolute protein concentrations and tracer kinetic data.

References

1. Jack, C.R., *et al.* Hypothetical model of dynamic biomarkers of the Alzheimer's pathological cascade. Lancet Neurol. 2010;9(1): 119–28.

2. Benilova, I., Karran, E., & De Strooper, B. The toxic Aβ oligomer and Alzheimer's disease: an emperor in need of clothes. Nat Neurosci. 2012;15(3):349–357.

3. Husain, M.M., Kenneth, T., Siddique, H., & McClintock, S.M. Present and prospective clinical therapeutic regimens for Alzheimer's disease. Neuropsychiatr Dis Treat. 2008;4(4):765–777.

4. Cole, S.L. & Vassar, R. The basic biology of BACE1: A key therapeutic target for Alzheimer's disease. Curr Genomics. 2007;8(8):509–530.

5. Dawkins, E. & Small, D.H. Insights into the physiological function of the β-amyloid precursor protein: beyond Alzheimer's disease. J Neurochem. 2014;129(5):756–69.

6. Wiltfang, J., *et al.* Higly conserved and disease-specific patterns of carboxyterminally truncated Aβ peptides 1-37/38/39 in addition to 1-40/42 in Alzheimer's disease and in patients with chronic neuroinflammation. J Neurochem. 2002;81(3):481–496.

7. Vingtdeux, V. & Marambaud, P. Identification and biology of α-secretase. J Neurochem. 2012;120 (Suppl. 1):34–45.

8. Willem, M., *et al.* η-Secretase processing of APP inhibits neuronal activity in the hippocampus. Nature. 2015;526(7573):443–7.

9. van Maanen, E.M.T., *et al.* Systems pharmacology analysis of the amyloid cascade after β-secretase inhibition enables the identification of an Aβ42 oligomer pool. J Pharmacol Exp Ther. 2016;357(1):205–16.

10. Bateman, R.J., Munsell, L.Y., Chen, X., Holtzman, D.M., & Yarasheski, K.E. Stable isotope labeling tandem mass spectrometry (SILT) to quantify protein production and clearance rates. J Am Soc Mass Spectrom. 2007;18(6):997–1006.

11. Potter, R., *et al.* Increased in vivo Amyloid-β42 production, exchange, and irreversible loss in Presenilin Mutations Carriers. Sci Transl Med. 2013;5(189):189ra77.

12. Patterson, B.W., *et al.* Age and amyloid effects on human central nervous system amyloid-beta kinetics. Ann Neurol. 2015;78 (3):439–453.

13. Cook, J.J., *et al.* Acute γ-secretase inhibition of nonhuman primate CNS shifts amyloid precursor protein (APP) metabolism from amyloid-β production to alternative APP fragments without amyloid-β rebound. J Neurosci. 2010;30(19):6743–50.

14. Bateman, R.J., *et al.* A gamma-secretase inhibitor decreases amyloid-beta production in the central nervous system. Ann Neurol. 2010;66(1):48–54.

15. Gilberto, D.B., *et al.* An alternative method of chronic cerebrospinal fluid collection via the cisterna magna in conscious rhesus monkeys. Contemp Top Lab Anim Sci. 2003;42 (4):53–59.

16. National Research Council. Guide for the Care and Use of Laboratory Animals The National Academies Press;Washington DC;1996.

17. Dobrowolska, J.A., *et al.* CNS amyloid-β, soluble APP-α and -β kinetics during BACE inhibition. J Neurosci. 2014;34(24): 8336–8346.

18. Wu, G., Sankaranarayanan, S., Hsieh, S.H.K., Simon, A.J., & Savage, M.J. Decrease in brain soluble amyloid precursor protein β (sAPPβ) in Alzheimer's disease cortex. J Neurosci Res. 2011;89(6):822–32.

19. Sankaranarayanan, S., *et al.* First demonstration of cerebrospinal fluid and plasma Aβ lowering with oral administration of a β-site amyloid precursor protein-cleaving enzyme 1 inhibitor in nonhuman primates. J Pharmacol Exp Ther. 2009;328(1):131–140.

20. Nubuo, I. & Hartmann, T. Analysis of Heterogeneous beta A4 Peptides in Human Cerebrospinal Fluid and Blood by a Newly Developed Sensitive Western Blot Assay. J Biol Chem. 1996;271(37):22908–22914.

21. Bauer, R.J. 2011 NONMEM users guide. Introduction to NONMEM 7.2.0 Technical report;ICON Development Solutions, Ellicott City, MD.

22. Wolfe, R.R. & Chinkes, D.L. Isotope tracers in metabolic research: principles and practice of kinetic analysis. 2nd ed. John Wiley & Sons;Hoboken, New Jersey;2005.

23. Gowrie, I., Roudsari, A., Umpleby, A., & Hovorka, R. Estimating Protein Turnover with a [15 N , 13 C] Leucine Tracer : a Study Using Simulated Data. J Theor Biol. 1999;198:165–172.

24. Cobelli, C., Saccomani, M.P., Tessari, P., Biolo, G., Luzi, L., & Matthews, D.E. Compartmental model of leucine kinetics in humans. Am J Physiol. 1991;261(4 Pt 1):E539–50.

25. Bonate, P.L. Pharmacokinetic-Pharmacodynamic Modeling and Simulation Springer;New York;2006.

26. Liu, K., Doms, R.W., & Lee, V.M.Y. Glu11 site cleavage and N-terminally truncated A beta production upon BACE overexpression. Biochemistry. 2002;41(9):3128–36.

27. Slemmon, J.R., *et al.* Measurement of Aβ1-42 in cerebrospinal fluid is influenced by matrix effects. J Neurochem. 2012;120(2): 325–33.

28. Matsumura, N., *et al.* γ-Secretase associated with lipid rafts: multiple interactive pathways in the stepwise processing of β-carboxyl-terminal fragment. J Biol Chem. 2014;289(8):5109–21.

Chapter 4

Supplemental Material

Supplement to

Integrating tracer kinetic data in a systems pharmacology model of the amyloid precursor pathway: effect of a β-secretase inhibitor

E.M.T. van Maanen, T.J. van Steeg, J.A. Dobrowolska Zakaria, M.S. Michener, M.J. Savage, M.E. Kennedy, R.J. Bateman, H.J. Kleijn, J.A. Stone, M. Danhof

SUPPLEMENTAL MATERIAL (1)

Kinetic Data Analysis of Plasma Enrichment

A kinetic model was developed to quantify plasma $^{13}C_6$-L enrichment in CMP rhesus monkeys. The results of the plasma enrichment analysis were included in the subsequent PK-tracer-PD analysis.

The kinetic model was developed and fitted to the data by means of non-linear mixed effects modeling using the NONMEM software package version 7 level 2 (see the Materials and Methods section in Chapter 4).

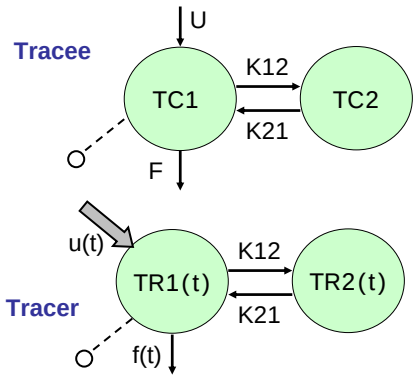

Figure S4.1: Model structure of kinetic model describing plasma tracer enrichment.
The model relates tracer input [mg/kg/hr] to the tracer-to-tracee ratio (TTR[%]). The model includes two tracee ($^{12}C_6$-Leucine) and two tracer ($^{13}C_6$-Leucine) compartments, representing extra- (pool 1) and intra-cellular (pool 2) tracee and tracer, respectively. Measurements are assumed to be taken from the extracellular compartment.
Dashed line: sampling. *Arrow*: tracer infusion. *U*: production of tracee in pool 1. *u(t)*: tracer infusion into pool 1. *F*: disposal of tracee from pool 1. *f(t)*: disposal of tracer from pool 1. *K12*: Transit rate from pool 1 to pool 2. *K21*: Transit rate from pool 2 to pool 1.

The compartmental model related the tracer infusion [mg/kg/h] to the measured enrichment, quantified as tracer ($^{13}C_6$-Leucine) to tracee (endogenous $^{12}C_6$-Leucine) ratio (TTR [%]), by describing tracee and tracer kinetics.

The model included two tracee ($^{12}C_6$-Leucine) and two tracer ($^{13}C_6$-Leucine) compartments (Supplemental Figure S4.1), representing extra- and intra-cellular tracee and

tracer. Measurements are assumed to be taken from the extracellular compartment.

Tracee is produced and disposed from tracee pool 1. Tracer is disposed from tracer pool 1. It is assumed that the natural production of tracer is negligible within the time frame of the experiment. The tracer coming into the system comes from the tracer infusion. The rate of disposal of tracer (f(t)) equals the rate of disposal of the tracee (*F*). The tracer and tracee kinetics is described by Eqs. S4.1 - Eqs. S4.4:

Tracee pool 1 (TC_1):

$$\frac{d}{dt}TC_1 = -K_{12} * TC_1 + K_{21} * TC_2 - F * TC_1 + U \tag{S4.1}$$

Tracee pool 2 (TC_2):

$$\frac{d}{dt}TC_2 = K_{12} * TC_1 - K_{21} * TC_2 \tag{S4.2}$$

Tracer pool 1 (TR_1):

$$\frac{d}{dt}TR_1(t) = -K_{12} * TR_1(t) + K_{21} * TR_2(t) - f(t) * TR_1(t) + u(t) \tag{S4.3}$$

Tracer pool 2 (TR_2):

$$\frac{d}{dt}TR_2(t) = K_{12} * TR_1(t) - K_{21} * TR_2(t) \tag{S4.4}$$

The TTR in plasma can then be calculated as described by Eqs. S4.5: Tracer to tracee ratio (*TTR*):

$$\frac{d}{dt}TTR = \frac{\frac{TR_1(t)}{TC_1} - TTR_{base}}{1 + 0.0111 * 6} * 100\% \tag{S4.5}$$

Here, TTR_{base} is the observed ratio of $^{13}C_6$-Leucine to $^{12}C_6$-Leucine prior to the addition of tracer.

The value 1/(1+0.0111*6) is the skew correction factor, accounting for the natural abundance of $^{13}C_6$-Leucine[1]. The spectrum of $^{13}C_6$-Leucine does not have the same mass abundance distribution as natural $^{12}C_6$-Leucine. In the calculation of TTR, this skew in

isotopomer distribution must be accounted for. The correction factor can be approximated by the value 1/(1+An), where A is the natural isotopic abundance of ^{13}C carbon atoms and n is the number of atoms labelled[2]. 1.11% of the naturally occurring carbon atoms are ^{13}C atoms and Leucine has six carbon atoms ($C_6H_{13}NO_2$), therefore 1/(1+0.0111*6).

The baseline of tracee pool 2 ($TC_{2\text{base}}$) and production of tracee (U) follow from steady state conditions.

$$TC_{2base} = TC_{1base} * \frac{K_{12}}{K_{21}} \tag{S4.6}$$

$$U = F * TC_{1base} \tag{S4.7}$$

Supplemental Table S4.1 shows all kinetic parameter estimates. All parameters could be estimated with good precision. For the baseline of the tracee pool 1 (TR_{1base}) interanimal variability was quantified. The model included a proportional error to describe the residual variability.

The measured plasma tracer enrichment was adequately described by the model, as can been seen from the visual predictive check (Supplemental Figure S4.2). Thus, the model could serve as input for PK-tracer-PD model analysis.

Table S4.1: Population parameter estimates including coefficient of variation (CV%) for kinetic model of plasma tracer enrichment.

PARAMETER	DESCRIPTION	VALUE	UNIT	CV%
F	Disposal	0.931	h^{-1}	25.5
K12	Transit rate from pool 1 to pool 2	0.644	h^{-1}	16.5
K21	Transit rate from pool 1 to pool 2	0.0154	h^{-1}	33.4
$TC_{1\text{base}}$	Baseline tracee pool 1	141	mg	15.1
$\omega^2_{TC_{1\text{base}}}$	Interanimal variability baseline tracee pool 1	0.0166		20.0
σ^2	Residual variability	0.722		20.4

Time to steady state

A simulation was performed with the kinetic model to investigate if plasma tracer enrichment reached steady state with the primed 12 h $^{13}C_6$-L infusion as used in the current SILK study (Supplemental Figure S4.3). To that end, the continuous infusion time was extended and the time to steady state derived. It takes approximately 52 days of infusion to reach steady state with the primed infusion technique. After approximately 10 and 17 days respectively 95% and 99% of the steady state level is reached. In the current study,

with the primed 12 h infusion, 62% of the steady state level of plasma tracer enrichment was reached.

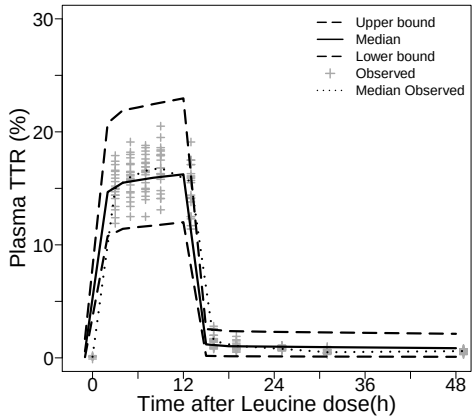

Figure S4.2: Visual predictive check of plasma tracer enrichment (TTR) time profile of $^{13}C_6$-Leucine in the rhesus with 90% confidence interval.

Observation sample size: n=260 from 5 monkeys collected over 2 days at four occasions.
Solid line: Median model predicted plasma TTR-time profile *Long-dashed line:* 90% prediction interval.
Dotted line: Median observed plasma TTR-time profile *Plus-symbols:* Observations.

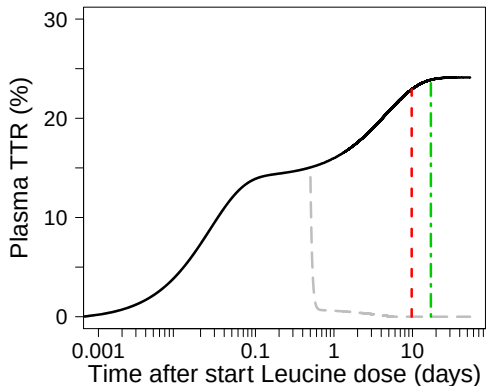

Figure S4.3: Simulation of plasma tracer enrichment (TTR) time profile using the identified kinetic model.
The plasma TTR is predicted after a primed infusion of 4 mg/kg bolus over 10 minutes, followed by 1300 h continuous infusion at a rate of 4 mg/kg/h, using the typical parameter estimates. Steady state plasma TTR is reached after $\sim$ 52 days of infusion.
Solid line: Model predicted plasma TTR-time profile after primed 1300 h infusion. *Long-dashed grey line:* Model predicted plasma TTR-time profile after primed 12 h infusion. *Dashed vertical red line:* Time of 95% steady state plasma TTR. *Dot-dashed vertical green line:* Time of 99% steady state plasma TTR.

References

1. Wolfe, R.R. & Chinkes, D.L. Isotope tracers in metabolic research: principles and practice of kinetic analysis 2nd ed. John Wiley & Sons;Hoboken, New Jersey;2005.
2. Rosenblatt, J., Chinkes, D., Wolfe, M., & Wolfe, R.R. Stable isotope tracer analysis by GC-MS, including quantification of isotopomer effects. Am J Physiol. 1992;263(3 Pt 1):E584–96.

SUPPLEMENTAL MATERIAL (2)

Table S4.2: Population parameters derived from model parameters for updated model based on ELISA and SILK data.

PARAMETER	DESCRIPTION	VALUE	UNIT
$A\beta40_{base}$ [a]	$A\beta40$ baseline	650.9	pM
$A\beta42_{base}$ [b]	$A\beta42$ baseline	23.92	pM
$FactorX_{base}$ [c]	FactorX baseline	1,015	pM
$sAPP\alpha_{base}$ [d]	$sAPP\alpha$ baseline	1,029	pM
$A\beta_{O\,base}$ [e]	$A\beta_O$ baseline	232.12	pM
APP_{base} [f]	APP baseline	2,179	pM
Rin_{APP} [g]	source of APP	$9.25*10^{-7}$	$L^{-1}h^{-1}$
Rin_{α} [h]	$sAPP\alpha$ formation rate	0.202	h^{-1}
Rin_{β} [i]	$sAPP\beta$ formation rate	0.209	h^{-1}
Kin_{40} [j]	$A\beta40$ formation rate	0.341	h^{-1}
Kin_{42} [k]	$A\beta42$ formation rate	0.0125	h^{-1}
Kin_x [l]	$A\beta x$ formation rate	0.122	h^{-1}

[a] $A\beta40_{base}$=$Fbase_{A\beta40}$*$sAPP\beta_{base}$.

[b] $A\beta42_{base}$=$Fbase_{A\beta42}$*$sAPP\beta_{base}$.

[c] $FactorX_{base}$=$Fbase_{FactorX}$*$sAPP\beta_{base}$.

[d] $sAPP\alpha_{base}$=$Fbase_{sAPP\alpha}$*$sAPP\beta_{base}$.

[e] $A\beta_{O\,base}$=Kpl*$A\beta42_{base}$/Krev.

[f] APP_{base}=$sAPP\beta_{base}$+$sAPP\beta_{base}$

[g] Rin_{APP}= (Rin_{α}+ Rin_{β})*APP_{base}*MW_{LeuL} /(TC_{1base}*10^9)

[h] Rin_{α}= $Rout_a$*$sAPP\alpha_{base}$/APP_{base}

[i] Rin_{β}= (Kin_{40}+Kin_{42}+Kin_x)*$sAPP\beta_{base}$/APP_{base}

[j] Kin_{40}=Kout*$A\beta40_{base}$/$sAPP\beta_{base}$

[k] Kin_{42}=Kin_{40}*$A\beta42_{base}$/$A\beta40_{base}$

[l] Kin_x=$Kout_x$*$FactorX_{base}$/$sAPP\beta_{base}$

SUPPLEMENTAL MATERIAL (3)

Simulation scale correction factor

In the PKPD model the plasma tracer enrichment was scaled to the level of tracer enrichment in the brain using a scale correction factor *FAC*. *FAC* represents the relative uptake of tracer in the precursor APP pool and was estimated to be 0.764. $^{13}C_6$-Leu does not achieve an isotopic equilibrium throughout all free pools of Leucine within the timeframe of the tracer infusion. Therefore, the tracer enrichment in the brain differs from plasma enrichment.

If isotopic equilibrium is assumed, and hence FAC=1, the fraction labelled protein is overestimated for fraction labeled total Aβ, sAPPβ and sAPPα, as is demonstrated in Supplemental Figure S4.4 for the placebo group.

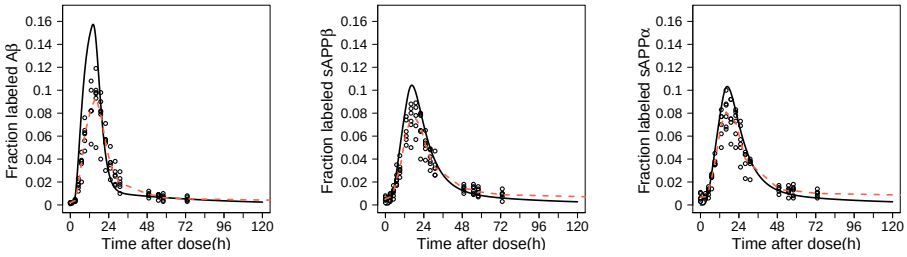

(A) fraction labeled total Aβ ***(B) fraction labeled sAPPβ*** ***(C) fraction labeled sAPPα***

Figure S4.4: Simulation fraction labelled protein response* vs. *time profile for the placebo group with scale correction factor (FAC) equals 1.
Solid line: Predicted fraction labelled protein response-time profile; *Dashed line:* Smoother through the observations of the placebo group; *Symbols:* Observations placebo group.

SUPPLEMENTAL MATERIAL (4)

Equations

The interaction between labeled and unlabelled APP, sAPPβ, sAPPα, Aβ40, Aβ42, Aβ_{O} and FactorX is described by Eq. S4.8 - Eq. S4.21:

$$\begin{aligned}\frac{d}{dt}APP^{unlab} =& Rin_{APP} * \frac{TC_1 * 10^9}{MW_{LeuU}} - (Rin\beta * EFF + Rin\alpha) * APP^{unlab} \\ & - Rin_{APP} * \frac{TR_1 * 10^9 * FAC}{MW_{LeuL}}\end{aligned} \tag{S4.8}$$

$$\begin{aligned}\frac{d}{dt}APP^{lab} =& Rin_{APP} * \frac{TR_1 * 10^9 * FAC}{MW_{LeuL}} \\ & - (Rin\beta * EFF + Rin\alpha) * APP^{lab}\end{aligned} \tag{S4.9}$$

$$\frac{d}{dt}sAPP\alpha^{unlab} = Rin\alpha * APP^{unlab} - Rout_a * sAPP\alpha^{unlab} \tag{S4.10}$$

$$\frac{d}{dt}sAPP\alpha^{lab} = Rin\alpha * APP^{lab} - Rout_a * sAPP\alpha^{lab} \tag{S4.11}$$

$$\begin{aligned}\frac{d}{dt}sAPP\beta^{unlab} =& Rin\beta * EFF * APP^{unlab} \\ & - (Kin_{40} + Kin_{42} + Kin_x) * sAPP\beta^{unlab}\end{aligned} \tag{S4.12}$$

$$\begin{aligned}\frac{d}{dt}sAPP\beta^{lab} =& Rin\beta * EFF * APP^{lab} \\ & - (Kin_{40} + Kin_{42} + Kin_x) * sAPP\beta^{lab}\end{aligned} \tag{S4.13}$$

$$\frac{d}{dt}A\beta_{40}^{unlab} = Kin_{40} * sAPP\beta^{unlab} - Kout * A\beta_{40}^{unlab} \tag{S4.14}$$

$$\frac{d}{dt}A\beta_{40}^{lab} = Kin_{40} * sAPP\beta^{lab} - Kout * A\beta_{40}^{lab} \tag{S4.15}$$

$$\frac{d}{dt}A\beta_{42}^{unlab} = Kin_{42} * sAPP\beta^{unlab} - Kout * A\beta_{42}^{unlab} - Kpl * A\beta_{42}^{unlab} + Krev * A\beta_{O}^{unlab} \tag{S4.16}$$

$$\frac{d}{dt}A\beta_{42}^{lab} = Kin_{42} * sAPP\beta^{lab} - Kout * A\beta_{42}^{lab} - Kpl * A\beta_{42}^{lab} + Krev * A\beta_{O}^{lab} \tag{S4.17}$$

$$\frac{d}{dt}A\beta_{O}^{unlab} = Kpl * A\beta_{42}^{unlab} - Krev * A\beta_{O}^{unlab} \tag{S4.18}$$

$$\frac{d}{dt}A\beta_{O}^{lab} = Kpl * A\beta_{42}^{lab} - Krev * A\beta_{O}^{lab} \tag{S4.19}$$

$$\frac{d}{dt}FactorX^{unlab} = Kin_x * sAPP\beta^{unlab} - Kout_x * FactorX^{unlab} \tag{S4.20}$$

$$\frac{d}{dt}FactorX^{lab} = Kin_x * sAPP\beta^{lab} - Kout_x * FactorX^{lab} \tag{S4.21}$$

The label incorporation in the APP pathway is informed from the kinetic model of plasma tracer enrichment. In Eqs. S4.8 and S4.9 this is imputed by TC_1 and TR_1, converted from mg to pM by $10^9/MW_{Leu}$. FAC in Eqs. S4.9 is a scale correction factor, used to scale the plasma tracer enrichment to the level of tracer enrichment in the brain.

The rate of change of APP with respect to time in the presence of the inhibitor is described by Eqs. S4.8 and S4.9, in which the BACE1 cleavage inhibition is incorporated by the factor *EFF*. *EFF* is the degree of inhibition caused by MBi-5, expressed as shown in Eqs. 5.8.

$$EFF = 1 - \frac{C_{\text{target}}^{\text{GAM}} * Imax}{C_{\text{target}}^{\text{GAM}} + IC50^{\text{GAM}}} \tag{S4.22}$$

Where C_{target} is the target site concentration of MBi-5 , *IC50* the C_{target} that results in 50% inhibition of BACE1, *Imax* is the maximum inhibition and *GAM* is the Hill coefficient. C_{target} was derived from the PK model as:

$$C_{\text{target}} = C_{\text{plasma}} * \frac{AUC_{\text{CSF}}}{AUC_{\text{plasma}}} \tag{S4.23}$$

Where AUC_{CSF} and AUC_{plasma} are the areas under the CSF and plasma concentration time curves, respectively. Here, C_{target} is assumed to follow the same profile as C_{plasma}, with the ratio

between the two concentrations being equal to the ratio between AUC_{CSF} and AUC_{plasma}.
It is assumed that the system is in steady state when no tracer and no treatment is given *(EFF=1)*. In addition, it is assumed that prior to tracer infusion, there are no labelled species. These steady state conditions were used to derive part of the system parameters.

From the steady state conditions and Eqs. S4.8 it follows that the source of APP *(*Rin_{APP}*)* was:

$$Rin_{APP} = (Rin\beta + Rin\alpha) * \frac{APP_{base} * MW_{LeuL}}{TC_{1base} * 10^9} \tag{S4.24}$$

Where APP_{base} is the baseline level of APP (*unlabelled, prior to tracer infusion*), which is assumed to be equal to the sum of the baseline levels of sAPPα and sAPPβ, as all alternate pathways are represented by the terms for α-secretase. BTC_1 is the baseline of tracee pool 1.
Using the steady state conditions and Eqs. S4.10 the sAPPα formation rate (*Rin*α), equivalent to the α-secretase cleavage step, can be derived:

$$Rin\alpha = Rout_a * \frac{sAPP\alpha_{base}}{APP_{base}} \tag{S4.25}$$

Where sAPPα_{base} is the baseline level of sAPPα.
The sAPPβ formation rate (*Rin*β), equivalent to the BACE1 cleavage step, follows from steady state conditions and Eqs. S4.12:

$$Rin\beta = (Kin_{40} + Kin_{42} + Kin_x) * \frac{sAPP\beta_{base}}{APP_{base}} \tag{S4.26}$$

Where $sAPP\beta_{\mathrm{base}}$ is the baseline level of sAPPβ.
From steady state conditions and Eqs. S4.14 the Aβ40 formation rate (*Kin40*), equivalent to a γ-secretase cleavage step can be calculated:

$$Kin_{40} = Kout * \frac{A\beta40_{base}}{sAPP\beta_{base}} \tag{S4.27}$$

Where $A\beta40_{\mathrm{base}}$ is the baseline level of Aβ40. $sAPP\beta_{\mathrm{base}}$ is the baseline level of sAPPβ, used here as surrogate for the baseline level of C99.
From Eqs. S4.16 and steady state conditions, with substitution of *Kout* from Eqs. S4.27, the Aβ42 formation rate (*Kin42*), equivalent to a γ-secretase cleavage step, is deduced:

$$Kin_{42} = Kin_{40} * \frac{A\beta42_{base}}{A\beta40_{base}} \tag{S4.28}$$

Where $A\beta42_{\mathrm{base}}$ is the baseline level of Aβ42.
From Eqs. S4.20 and steady state conditions, the FactorX formation rate (*Kinx*) is deduced:

$$Kin_x = Kout_x * \frac{FactorX_{base}}{sAPP\beta_{base}} \tag{S4.29}$$

Where $FactorX_{\mathrm{base}}$ is the baseline level of FactorX.

The model structure includes two times six transit compartments, two for each biomarker (labelled and unlabelled) (sAPPα, sAPPβ, Aβ40, Aβ42, Aβ_{O}, FactorX), to account for transport from the target site in the brain to CSF. These transit processes are described, in general, by Eqs. S4.30 and S4.31:

$$\frac{d}{dt} species_{CSF}^{lab} = Kt * (species^{lab} - species_{CSF}^{lab}) \tag{S4.30}$$

$$\frac{d}{dt} species_{CSF}^{unlab} = Kt * (species^{unlab} - species_{CSF}^{unlab}) \tag{S4.31}$$

Where *Kt* is the transit rate for the particular species (*KtAP* for sAPPα and sAPPβ; *KtAB* for Aβ40, Aβ42 and Aβ_{O}; *KtX* for FactorX).

The fraction labelled species (FracLab) for each APP metabolite in CSF are calculated as labelled over total species (Eq. S4.32-S4.34).

$$FracLab_{sAPP\alpha_{CSF}} = \frac{sAPP\alpha_{CSF}^{lab}}{sAPP\alpha_{CSF}^{Total}} \tag{S4.32}$$

$$FracLab_{sAPP\beta_{CSF}} = \frac{sAPP\beta_{CSF}^{lab}}{sAPP\beta_{CSF}^{Total}} \tag{S4.33}$$

$$FracLab_{A\beta_{CSF}} = \frac{A\beta_{40CSF}^{lab} + A\beta_{42CSF}^{lab} + A\beta_{O_{CSF}}^{lab} + FactorX_{CSF}^{lab}}{A\beta_{40CSF}^{Total} + A\beta_{42CSF}^{Total} + A\beta_{O_{CSF}}^{Total} + FactorX_{CSF}^{Total}} \tag{S4.34}$$

The total concentrations for each APP fragment in CSF are calculated as:

$$Total_{species_{CSF}} = species_{CSF}^{lab} + species_{CSF}^{unlab} \tag{S4.35}$$